

1 **The Role of Local Topography and Sea Surface Temperature on Summer**
2 **Monsoon Precipitation over Bangladesh and North-East India**

3
4 Abdullah A. Fahad*^{1,5}, Bohar Singh², Mostofa Kamal^{3,5}, Tanvir Ahmed^{4,5}, MD. Minhazul
5 Kibria⁵, Nazimur Rashid Chowdhury⁵

6
7 ¹Global Modeling and Assimilation Office, NASA GSFC, Greenbelt, MD, USA

8 ²International Research Institute for Climate and Society, Columbia University, NY, USA

9 ³School of Environment and Sustainability, GIWS, University of Saskatchewan, Saskatchewan, Canada

10 ⁴School of Earth and Environmental Sciences, Seoul National University, Seoul, South Korea

11 ⁵Department of Physics, Shahjalal University of Science & Technology, Sylhet, Bangladesh

12
13 **Keywords:** Asian monsoon, Rainfall, Topography, Bangladesh, Bay of Bengal, Moisture flux

14
15
16
17 * **Corresponding Author:** Abdullah A. Fahad, NASA Goddard Space Flight Center. Email:
18 a.fahad@nasa.gov, Address: 8800 Greenbelt Rd, Greenbelt, MD 20771.

19
20
21
22
23
24
25
26
27
28
29
30
31
32

33
34
35
36
37
38
39
40
41
42
43
44
45
46
47
48
49
50
51
52
53
54
55
56
57
58

Abstract

Bangladesh receives most of its precipitation from June to September in the form of rainfall as a part of the Asian summer monsoon system. Bangladesh is a relatively flat region, surrounded by the southern Himalayas and Meghalaya Plateau in the north, Arakan Mountains in the east, and the Bay of Bengal (BOB) in the south. Although several studies have investigated the mechanisms that drive the Asian monsoon precipitation, very few studies have focused on the monsoon precipitation in Bangladesh. This study investigated the influence of the topography of the surrounding regions and sea surface temperature on the summer monsoon precipitation of Bangladesh and the surrounding regions. Using observed data, we showed that moisture convergence near the mountains contributes to the precipitation of Bangladesh, whereas the BOB acts as a source of moisture. A strong low-level jet carries the moisture inland as the land–sea thermal contrast intensifies the wind circulation during the summer. Three differently forced simulations of the Euro-Mediterranean Centre on Climate Change coupled climate model (CMCC CM2) were analysed to investigate the influence of the surrounding region's topography and sea surface temperature on the summer monsoon precipitation. The low-resolution simulation showed no spatial variability of precipitation and dry bias due to the overly smooth topographical representation of mountains. The high-resolution coupled simulation, with a better representation of topography, improved the moisture convergence at the foothills and precipitation bias. The high-resolution prescribed sea surface temperature further improved the precipitation bias by intensifying the low-level jet that transports moisture over Bangladesh.

1. Introduction

59
60
61
62
63

As part of the South Asian Monsoon system, Bangladesh receives 70-75% of its annual precipitation as rainfall from June to September months (June-July-August-September or JJAS) (Ahmed 1993; Ahmed et al. 2020) (Fig. 1). Bangladesh is a flat region occupied by the Ganges-

64 Brahmaputra-Meghna delta and surrounded by the Arakan Mountains in the east, Meghalaya
65 Plateau in the northeast, and southern foothills of the Himalayas in the north (Fig. 2a). Realistic
66 simulation of Bangladesh's seasonal mean monsoon (June-September) has proven to be a
67 challenging task for state-of-the-art climate models due to many factors, including the surrounding
68 complex topography, large sea surface temperature (SST) variability in the BOB, and
69 representation of the convection in the state-of-the-art climate models (Lucas-Picher et al. 2011;
70 Xie et al. 2006). The northeast region of Bangladesh (i.e., the Sylhet division) and its surrounding
71 regions (Cherrapunjee, Mawsynram, and Meghalaya Plateau of India) is the wettest region on earth
72 (Murata et al. 2017). The zonal distribution of observed precipitation also shows that Bangladesh's
73 southeastern and northwestern regions receive the most precipitation during the summer monsoon
74 (Fig. 1c). The latest General Circulation Models (GCM)s still have significant precipitation biases
75 over these regions, mainly in low-resolution climate models (Oouchi et al., 2009; Cherchi and
76 Navara, 2007). A low vertical and horizontal resolution in simulations do not adequately represent
77 the actual complex variations in the topography of the earth's surface. In the atmosphere, moist air
78 needs to reach the cloud condensation level to form precipitation. Uplift is a forcing mechanism
79 that can transport boundary layer moisture to the cloud condensation level in the atmosphere. The
80 natural lifting mechanisms include differential surface heating and air mass boundaries (fronts and
81 dry lines), whereas the mechanical lifting mechanism includes steep topography such as
82 mountains. Due to coarse spatial resolution, most GCMs cannot represent correct orographic
83 lifting, resulting in an erroneous precipitation simulation.

84 The role of topography in modulating the South Asian monsoon has been studied widely (Hahn
85 and Manabe 1975; Chakraborty et al. 2006; Gill 1980; Yanai and Li 1994; Kitoh 2002; Privé and
86 Plumb 2007a, b; Goswami 2010; Prokop and Walanus 2015). Hahn and Manabe (1975)
87 investigated the role of mountains in South Asian monsoon circulation. They used a numerical
88 climate model with 11 vertical levels, 270 km horizontal resolution, and prescribed SST to explore
89 the contribution of local mountains to the global atmospheric circulation pattern. Two sets of
90 experiments were done in their study to compare with the observations: (1) South Asian monsoon
91 simulation with Asian mountains present, and (2) without Asian mountains in the climate model.
92 Results showed that the South Asian summer monsoon was well simulated with mountains present
93 in the climate model compared to the numerical experiment with no mountains. The low-level

94 circulation (1000hPa geopotential height) showed a strong low-pressure circulation near the
95 Tibetan Plateau with mountains present. In contrast, there was no clear pattern of the low-pressure
96 system over South Asia without mountains in the Hahn and Manabe (1975) experiments. However,
97 these experiments were done in a GCM with a low horizontal and vertical resolution. The
98 surrounding topography of Bangladesh (e.g., Meghalaya Plateau and Arakan mountains), or
99 elsewhere, was unaccounted for even in the experiments with mountains. As a result, no intense
100 precipitation was generated over Bangladesh and its surrounding regions (e.g., Meghalaya Plateau)
101 during the summer monsoon, where observed data shows a high intensity of summer monsoon
102 precipitation.

103

104 Investigating the role of the Tibetan Plateau on local precipitation, Boos and Kuang (2010) found
105 that diabatic heating over the Tibetan Plateau intensifies the precipitation near the southern edge
106 of the Himalaya range. The Himalayan range supports a strong monsoon circulation by preventing
107 the mixing of dry extratropical air into the warm and moist air over continental India. Later, Boos
108 and Hurley (2013) showed that the Coupled Model Intercomparison Project Phase (CMIP) 3 and
109 5 models exhibit common biases in thermal structure over South Asia during the Boreal summer
110 monsoon season due to an overly smooth topographic representation in the climate models.
111 Recently, Acosta and Huber (2020) showed that high-resolution climate models accurately
112 represent the topographic and atmospheric dynamics interactions. The Himalayas and the Tibetan
113 Plateau play an important role in redirecting moisture convergence to produce local orographic
114 precipitation, while the SST gradient mainly govern large-scale circulations, advecting water vapor
115 onshore regardless of the topographical feature. Focusing on the northeastern region of the
116 Himalayas, Gu et al. (2020) further confirmed that a high-resolution Regional Climate Model
117 (RCM) simulation significantly decreases precipitation bias over the Brahmaputra River basin.
118 The convective system is a crucial mechanism that contributes to the monsoon precipitation in a
119 region like Bangladesh and its surrounding regions by interacting with the local topography
120 (Romatschke et al. 2010; Goswami et al. 2010; Medina et al. 2010). Convective cells associated
121 with the BOB depression evolve into mesoscale convective systems near the eastern Himalayas to
122 be lifted by the local topography triggering precipitation (Medina et al. 2010). Using the Weather
123 Research and Forecasting (WRF) model, Konduru & Takahashi (2020) showed that the diurnal
124 cycle and precipitation variation over the Indian monsoon region significantly depends on the

125 horizontal resolution of simulation compared to the convection scheme used in the model. Besides
126 the representation of orography, slowly varying local and remote SST patterns are also crucial for
127 a realistic representation of monsoons in GCM's (Shukla, 1981).

128
129 Several studies have shown that the North Indian Ocean (the Arabian Sea and the BOB), Atlantic,
130 and Pacific Ocean SST play a role in modulating Indian summer monsoon precipitation variability
131 (Breitenbach et al. 2010; Kumar et al. 2013; Preethi et al., 2010; Roxy 2014; Cherchi et al., 2018;
132 Ratna et al., 2016; Feng et al., 2018; Singh et al., 2019). Rao and Goswami (1988) found that the
133 correlation between monsoon precipitation and SST is not static rather it varies throughout the
134 season. They also noticed a strong positive correlation during pre-monsoon, a significantly
135 negative correlation during post-monsoon, and a small correlation during peak monsoon. Goswami
136 et al. (2016) found that the ocean components of most current coupled models fail to reproduce
137 the BOB's upper ocean thermal structure because of a poor representation of mixing between
138 highly fresh and stratified regions. High-resolution and high-frequency observations are required
139 to understand the interaction between Indian Ocean dynamics and Indian summer monsoon
140 precipitation (George et al., 2016; Goswami et al., 2016). Roxy (2014) found a statistically
141 significant relationship between SST and a linear increase in precipitation up to 31 °C for the Asian
142 summer monsoon. The study quantified a ~2 mm/day increase in rainfall for a 1 °C increase in
143 SST. Kumar et al. (2013) found that different reanalysis data show a varying degree of strength in
144 the SST-precipitation relationship. The influence of SSTs on the precipitation of Bangladesh and
145 its surrounding regions is also documented in several studies (Salahuddin et al., 2006;
146 Wahiduzzaman et al., 2021). Alapaty et al. (1995) found that Indian Summer Monsoon
147 precipitation is sensitive to the SST distribution of the BOB. Their study found that there is
148 approximately a 20% increase in the evaporation and a 10% increase in the precipitation with the
149 observed SST compared to the model's SST. The authors also noticed a one to two-degree increase
150 in the SST over some parts of the BOB and the Arabian Sea, leading to a pressure drop of 2 to 3
151 hPa and increased wind speed. Yang et al. (2017) show that an atmospheric river connected to the
152 BOB leads to extreme precipitation over northern India during the summer monsoon season.

153
154 Krishnamurthy and Goswami (1999) found a strong relationship between the interdecadal
155 variability of the Indian summer monsoon precipitation and interdecadal variations of multiple

156 ENSO indices. In an interannual timescale, Chowdhury (2003) showed that seasonal flooding over
157 Bangladesh is significantly related to the Southern Oscillation Index (SOI) instead of El-Nino
158 Southern Oscillation (ENSO). Chowdhury (2003) found that a positive phase of the SOI leads to
159 dry conditions over Bangladesh, whereas the negative phase is linked with wet conditions over
160 Bangladesh. Ahmed et al. (2017) investigated long-term precipitation trends over Bangladesh
161 during the summer monsoon season and analyzed the relationship between precipitation over
162 Bangladesh and SST modes of variability, such as Indian Ocean Dipole (IOD) and ENSO, and
163 noticed that a positive phase of IOD has a significant relationship with the summer monsoon
164 precipitation of Bangladesh. Mishra et al. (2017) found a linkage between phases of the Madden–
165 Julian Oscillation (MJO) and precipitation over the Meghalaya plateau. Phase 1 and 2 of the MJO
166 circulation creates a strong moisture convergence near the Meghalaya plateau, leading to
167 intensified precipitation over northeast India and the northern Bangladesh region during the
168 summer monsoon. Several studies have also reported that changes in soil moisture contribute to
169 the pre-monsoon and monsoon precipitation variation over Bangladesh (Ono & Takahashi, 2016;
170 Sugimoto & Takahashi, 2017)

171
172 Several studies have investigated precipitation variability over Bangladesh using Regional Climate
173 Models (RCMs). RCMs have relatively higher resolution compared to GCMs. However, RCMs
174 lack two-way interactions with the large-scale circulation, in contrast to GCMs. This property of
175 RCMs can lead to model biases in the local atmospheric circulation and precipitation. Using large
176 ensembles of RCM simulations, Picher et al. (2011), Nowreen et al. (2015), and Rimi et al. (2019)
177 showed that there are significant dry biases present all over Bangladesh with maximum bias over
178 the north-east and southeast regions. A study conducted by Islam et al. (2008) found that an RCM
179 overestimates precipitation in the pre-monsoon and winter seasons. In contrast, it underestimates
180 the precipitation in the monsoon season using the Providing Regional Climates for Impacts Studies
181 (PRECIS) model. After analyzing the results of RCMs, Feng and Fu (2006) concluded that RCMs
182 improve the simulation of the spatial pattern of precipitation but not the intensity. Since RCMs use
183 initial and lateral boundary conditions from a GCM, a significant part of the uncertainty of the
184 RCM-simulated precipitation can be traced back to input from the GCM (Syed et al., 2014).
185 Therefore, proper representation of topographic features and reliable GCM boundary conditions
186 for RCMs can help in simulating the long-term precipitation climatology over this region.

187

188 Although several studies have shown how precipitation during the summer monsoon is a unique
189 feature over Bangladesh and its surrounding regions, very few studies have focused on the physical
190 mechanisms that drive the climatological summer monsoon precipitation over Bangladesh and its
191 surrounding regions (Rafiuddin et al. 2010; Abdullah et al. 2020). Most studies have focused on
192 extreme precipitation events on short timescales that don't necessarily determine the seasonal mean
193 precipitation of the region. Studies that explore the influence of local topography on local
194 precipitation lack attention to the northeastern and southern parts of Bangladesh and focus broadly
195 on the Indian summer monsoon. Within the common framework of forcing RCMs with GCM
196 boundary conditions, it is crucial to understand what generates precipitation variability over
197 Bangladesh in the first place.

198

199 The objective of the study is to understand the role of the topography and SST in summer monsoon
200 precipitation over Bangladesh and its surrounding regions in hierarchical climate model
201 simulations from CMIP6 experiments. The organization of this paper is structured as follows:
202 section (2) describes the various datasets and their evaluation methodologies, section (3) presents
203 results, and section (4) provides a detailed discussion of the findings of the study and compares
204 them to other published studies. Finally, section (5) summarizes the key findings of this study.

205

206 **2. Data and Methodology**

207

208 We analyzed various observational and numerical model simulated datasets, including observed
209 gridded precipitation, topographic distribution, and various GCM datasets under the CMIP6
210 project. This study examined 34 years of common data for calculating model biases, and the
211 observed data were interpolated to the model's resolution to find model biases.

212

213 To explore the characteristics of the summer monsoon precipitation over Bangladesh, we used the
214 Climate Hazards Group InfraRed Precipitation with Station data (CHIRPS) observed high
215 resolution gridded dataset version 2 (Funk et al. 2015, Montes et al. 2021). CHIRPS uses 0.05°
216 resolution satellite imagery and in-situ station data to create gridded precipitation time series
217 spanning 50° South to 50° North, and data from 1981 to the near present. To test our hypothesis

218 about the precipitation mechanism, we used observed SST data HadISST (Rayner et al., 2003).
219 For the zonal wind U, meridional wind V, and specific humidity q, the reanalysis dataset ERA5 is
220 used in this study (Hersbach et al. 2020). The observed surface height of the topography of
221 Bangladesh and its surrounding regions was collected from Global Multi-resolution Terrain
222 Elevation Data (GMTED2010) to make a comparison with the model's topography (Fig. 2a)
223 (Danielson, J.J., Gesch 2011). The resolution of the surface height topography data is
224 $0.008^{\circ} \times 0.008^{\circ}$.

225

226 To further investigate the contribution of local topography and SST, we used present-day climate
227 simulation of GCM CMCC CM2 (Cherchi et al. 2019), which participates in the CMIP6 project
228 (Eyring et al. 2016). The CMCC CM2 is a global coupled model primarily based on the
229 Community Earth System Model (CESM) project (<http://www.cesm.ucar.edu>), and is developed
230 and maintained by the Euro-Mediterranean Centre on Climate Change (CMCC) to understand
231 global climate variability and climate change.

232

233 To quantify the influence of local topography versus SST we used three model simulations of
234 CMCC CM2 from CMIP6 project: (1) a coupled simulation with low resolution (Lowres)
235 atmosphere ($1^{\circ} \times 1^{\circ}$) and high-resolution ocean ($0.25^{\circ} \times 0.25^{\circ}$), (2) a coupled simulation with high-
236 resolution (Highres) atmosphere ($0.25^{\circ} \times 0.25^{\circ}$) and high-resolution ocean ($0.25^{\circ} \times 0.25^{\circ}$), and (3) a
237 AGCM simulation with high-resolution (Highres SST) atmosphere ($0.25^{\circ} \times 0.25^{\circ}$) and prescribed
238 observed SST (HadISST $0.25^{\circ} \times 0.25^{\circ}$). The Lowres simulation was taken from the CMIP6
239 Historical run, the Highres simulation was taken from the CMIP6-HighresMIP Hist-1950 run, and
240 the Highres SST simulation was taken from the CMIP6-HighresMIP highresSST-present run.
241 Compared to the Lowres simulation, the HighresMIP model simulations (Highres and Highres
242 SST) have a higher resolution of topographical features (Haarsma et al., 2016). The Lowres
243 coupled run uses the Community Atmospheric Model 4 as the atmospheric model with 30 vertical
244 levels and the NEMO3.6 as the ocean model. The Highres coupled run uses a similar configuration,
245 except the atmospheric model is in a higher resolution with a better-resolved topography. The
246 Highres SST is an AGCM run where the ocean is prescribed SST from observed HadISST data
247 with a high-resolution atmospheric model. All three simulations use the same aerosol, land surface,
248 and ocean bio-geochemistry model.

249
 250 Gao et al. (2012) investigated the sensitivity of moisture flux convergence to the choice of model
 251 grid resolution and found that a high-resolution model better simulates moisture flux convergence
 252 on the windward side of the mountains because of a more realistic representation of hydrodynamic
 253 instabilities. Seager et al. (2007) considered the vertically integrated moisture flux convergence as
 254 the net precipitation in the long term. Given the complex topographic distribution of the
 255 Himalayas, Arakan mountains, and the Meghalaya Plateau, it is imperative to investigate the role
 256 of model resolution to moisture flux convergence and precipitation climatology over Bangladesh
 257 and its surrounding regions. We computed the Vertically Integrated Moisture Flux (VIMF) as seen
 258 in Equation 1 (Darand and Pazhoh, 2019).

259
 260
$$VIMF = \frac{1}{g} \int_{P_s}^{P_t} \left(\frac{\partial uq}{\partial x} + \frac{\partial vq}{\partial y} \right) \cdot dP, \dots \dots \dots (1)$$

261
 262 Where q is the specific humidity, P_s is surface pressure (in our study 1000 hPa), P_t is the pressure
 263 at the atmospheric level up to which lower troposphere moisture flux is calculated (in our study
 264 700 hPa), u and v are the x- and y-components of the wind, respectively, and g is the acceleration
 265 due to gravity. The unit of VIMF is $\text{kg m}^{-2}\text{s}^{-1}$. A positive value of VIMF indicates that the moisture
 266 is spreading out or diverging, and a negative value suggests the moisture is concentrating or
 267 converging.

268
 269 Earlier studies show that the Vertically Integrated Moisture Transport (VIMT) flux from the Indian
 270 Ocean supplies a significant amount of moisture for the Asian summer monsoon precipitation
 271 (Chansaengkachang et al., 2018; Ullah and Gao, 2012; Fasullo and Webster 2003). The moisture
 272 for the monsoon precipitation over Pakistan primarily originates from the Arabian Sea, and the
 273 BOB plays a secondary role (Ullah and Gao, 2012). In contrast, the BOB is the dominant source
 274 of moisture for precipitation in Bangladesh. The VIMT from the Arabian sea contributes
 275 minimally to the precipitation over Bangladesh because most of the humidity directed in the
 276 northeasterly direction condense and precipitate on the windward side of the Western Ghats
 277 mountains and over it. Thus, our study focused on assessing the VIMT from the BOB, and we
 278 calculated the VIMT (Equation 2) as defined by Fasullo and Webster (2003).

279

280
$$VIMT = \int_{surface}^{700\text{ mb}} q \mathbf{U} \cdot d\mathbf{P}, \dots\dots\dots (2)$$

281
282 Where q is the specific humidity and \mathbf{U} is the wind vector.

283
284 Finally, we achieved our research objective of finding the isolated influence of the SST and
285 topography on the summer monsoon precipitation of Bangladesh by analyzing CCMC CM2 from
286 CMIP6 HighresMIP simulations forced with different resolutions of topography and prescribed
287 SST.

288
289 **3. Results**

290
291 **3. 1. Observed Summer Monsoon Precipitation over Bangladesh**

292
293 During JJAS, there are three maximum precipitation regions over Bangladesh (Fig. 2a). The
294 northeastern part of Bangladesh (the Sylhet division and the surrounding Indian states) receives
295 the maximum precipitation during the summer monsoon, along with the northwestern region of
296 Bangladesh (northern Rangpur division) and their surrounding Indian regions. The other region of
297 Bangladesh that receives excessive precipitation during the summer monsoon is southeastern
298 Bangladesh (Chittagong division) and its surrounding regions (Arakan state, Myanmar and
299 Tripura, and Mizoram states of India). The unique precipitation pattern over Bangladesh and its
300 surrounding regions during both annual mean and JJAS mean is primarily dominated by the
301 surface topographical features (Fig. 1 & Fig. 2). In other words, the three maximum precipitation
302 regions of Bangladesh are directly associated with nearby mountains. For example, the
303 northeastern region of Bangladesh receives >25 mm/day precipitation during the summer
304 monsoon, and the pattern of precipitation is associated with the area of the Meghalaya Plateau.
305 The magnitude of the precipitation maxima over the northwestern region is nearly 22 mm/day
306 precipitation during the summer monsoon and is associated with the southern Himalayan Mountain
307 range (Fig. 2). The high precipitation band over Bangladesh's southeastern and eastern parts
308 depicts 20-25 mm/day precipitation. It is associated with the mountain band over the Myanmar
309 and Indian state, known as Arakan Mountains.

310

311 The VIMF divergence from ERA5 reanalysis showed that areas of high precipitation over
312 Bangladesh and its surrounding regions result from strong lower tropospheric moisture
313 convergence (Fig. 2b). The topography of the mountain bands forces the lower tropospheric
314 moisture flux convergence over northern and northeastern Bangladesh, thus generating high
315 precipitation. The VIMF also diverges in the lower troposphere over the BOB, located in the south
316 of Bangladesh (Fig. 2b). The strong divergence of moisture flux over the BOB acts as a source of
317 moisture that is transported by the low-level jet (LLJ) stream to the mountainous regions. The 925
318 hPa wind circulation shows that lower-level air travels from the southwest of the BOB to the
319 northern part of Bangladesh, and then moves toward the northeast and northwest of Bangladesh
320 near the southern Himalayan mountains. The Meghalaya plateau and south Himalayan Mountain
321 range block the lower-level wind circulation and force moist air to converge and get lifted due to
322 mechanical lifting, leading to precipitation (Fig 2b). The Arakan mountain and Meghalaya Plateau
323 form a concave geometry with vertex over the Sylhet division (Fig. 2a). The Himalayas and Arakan
324 mountain range lie along the northern and eastern borders (perpendicular and parallel) of
325 Bangladesh. Due to the distinct geometry of these three regions, the LLJ coming from the BOB
326 intersects at three different angles. It contributes to the moisture convergence over maximum
327 precipitation regions of northern and northeastern Bangladesh. The LLJ reaches a climatological
328 maximum during the local summer monsoon due to a maximum land-sea thermal contrast. The
329 near-surface temperature and lower troposphere air temperature increases faster than the ocean due
330 to the local monsoon heating and relatively higher ocean heat capacity during JJAS. This process
331 creates a higher land-sea thermal contrast during the summer monsoon that drives the LLJ stream
332 and transports moisture along with it. The lower-level wind circulation of the LLJ is parallel to the
333 Arakan mountains. A stronger VIMT (Fig 2c) and weaker moisture convergence over the southeast
334 region of Bangladesh suggest that the precipitation maxima over southeastern Bangladesh are due
335 to a direct moisture convergence rather than the topographical features of the region.

336

337 **3. 2. Numerical Experiments Decomposing the Influence of Topography & SST**

338

339 The seasonal cycle of the domain-averaged precipitation of Bangladesh is shown in the Fig. 4. The
340 result shows the Highres significantly improves the seasonal cycle of the precipitation, whereas
341 the Highres SST further improves the seasonal cycle compared to the Lowres CMCC CM2

342 simulation. The total area-averaged monthly mean precipitation and the peak of seasonal cycles
343 are enhanced in the Highres SST simulations compared to the Lowres and Highres model
344 simulations. Onset, cessation, and length of the rainy season of the summer monsoon are also
345 improved in the Highres SST model simulation as compared to the other two model simulations.
346 This comparison suggests that the SST has significant influence over the summer monsoon
347 precipitation. However, the magnitude of the seasonal precipitation is still underestimated when
348 compared to the observations. The CMCC CM2 climate model shows significantly different
349 summer monsoon precipitation climatology over Bangladesh with specific configurations (Figs.
350 3, 4, & 5). The Lowres simulation shows no clear precipitation maxima over Bangladesh with 4-6
351 mm/day precipitation (Fig 5a), due to a nonexistent topographical feature over the regions that
352 surrounds Bangladesh (Fig. 3a). In contrast, the Highres model simulation shows a spatial
353 variability of precipitation with maxima over the Meghalaya Plateau that extends to the
354 northeastern part of the Bangladesh (Sylhet division), precipitation maxima over the northwest of
355 Bangladesh (over Indian state, near southern Himalayan Mountain range), and maxima over the
356 southeastern part of Bangladesh that extends to the Arakan mountains (Fig. 5b). The Highres
357 model shows a better spatial pattern of precipitation distribution than the Lowres due to a better
358 topographic resolution (Fig. 3b). Seasonal mean precipitation is increased over the flat land of
359 Bangladesh from 4 mm/day to ~10 mm/day in Highres model simulations (Fig. 5b), as compared
360 to the Lowres model simulation (Fig. 5a). In the Highres SST, spatial precipitation pattern is further
361 improved especially in the southern and southeastern Bangladesh region.

362

363 The bias in the precipitation simulation of the CMCC CM2 model simulation when compared to
364 the observation shows that the Lowres model has the maximum model bias in both the spatial
365 pattern and magnitude of precipitation over Bangladesh and its surrounding regions (Fig. 5d). The
366 Lowres model simulation shows an underestimation of precipitation with a maximum bias of 15
367 mm/day over northeastern Bangladesh (Fig. 5d). The precipitation bias is maximum near the
368 Arakan Mountains and Meghalaya Plateau, where climatological precipitation has an observed
369 maximum (Fig. 5a). The Highres model simulation's precipitation bias is significantly lower than
370 the Lowres simulation (Fig. 5e). The Highres simulation still shows significant precipitation biases
371 over northeastern and southeastern Bangladesh in regions of heavy climatological precipitation
372 (Fig. 5e). These dry biases in the Highres are due to the false maxima (wrong maximum

373 precipitation region) of precipitation on the Highres simulation over these two regions, especially
374 over the northeastern Bangladesh (Fig. 5e). Observations show maximum precipitation over the
375 northeastern districts of Bangladesh (Sylhet division) (Fig. 2a), whereas the CMCC CM2 produces
376 maximum precipitation over India near the Meghalaya Plateau (Fig. 3b, 5b, & 5e). The Highres
377 simulation of the CMCC CM2 shifts the precipitation maximum towards the north over the
378 northeastern Bangladesh (Fig. 3b & 5b). This particular model bias occurs due to the Meghalaya
379 Plateau not being well-represented in the Highres model simulation (Fig. 2b & Fig. 3b). The
380 Highres SST simulation shows significantly lower summer monsoon precipitation bias in the
381 southeastern Bangladesh than the Lowres and Highres coupled simulations (Fig.5f). Reduction of
382 the precipitation bias over the southeastern Bangladesh in the Highres SST compared to Highres
383 coupled model simulations suggest that the SST in the BOB and tropical ocean system plays an
384 important role in the summer monsoon precipitation simulation in Bangladesh. Interestingly, the
385 precipitation bias pattern is similar in the Highres SST and Highres simulation due to the same
386 model topography (Fig. 5f).

387

388 In this section, we have analyzed VIMF convergence and transport to understand the role of the
389 topography of the surrounding regions and SST in the simulation of seasonal mean precipitation
390 over Bangladesh. There is a significant bias (compared to the observation) in the VIMF over almost
391 all of Bangladesh and its surrounding regions (Fig. 6 & 7). Due to a lack of well-resolved
392 topography, the Lowres simulation shows a maximum bias in the moisture flux in terms of spatial
393 pattern and magnitude (Fig. 6a & 6d). The Highres simulates a more realistic moisture flux
394 convergence due to a better topography; however, the magnitude of the moisture flux is still
395 significantly underestimated (Fig. 6b & 6e). A similar bias pattern in the VIMF convergence is
396 seen in the Highres SST simulation (Fig. 6c & 6f). The similarity in VIMF convergence in the
397 Highres coupled and Highres SST indicates that moisture flux convergence near the mountains of
398 the surrounding regions is mostly dominated by the topography rather than the SST variability.
399 Interestingly, over the northeastern Bangladesh and surrounding regions in the CMCC CM2
400 produces a strong moisture convergence only over the Meghalaya plateau, which results in a false
401 precipitation maximum in the model (Fig. 6e). These false precipitation maxima are also present
402 in the Highres SST, as both simulations use similar atmospheric model resolution and topography
403 (Fig. 6f). However, the intensity of the moisture transport in the Highres SST due to a realistic

404 SST is related to a better LLJ circulation and higher moisture content (Fig. 6f). The VIMT of the
405 CMCC CM2 simulations is shown in Fig. (7). The precipitation bias over Bangladesh and its
406 surrounding regions is also due to a model bias in the simulation of low-level moisture transported
407 from the BOB over land (Fig. 7). The Lowres simulation shows underestimated moisture transport
408 over almost the entire Bangladesh land regions (Fig. 7a & 7d), and overestimated moisture
409 transport on the east side of the mountains in the surrounding regions due to an overly smooth
410 representation of the local topography. In the Highres coupled model simulation, the
411 underestimation of moisture transport over the Bangladesh land region remains similar. However,
412 the overestimation of moisture transport is improved in the east of the mountains of the
413 surrounding regions due to an improved topographical representation. The Highres SST produces
414 stronger moisture transport, leading to a lowest precipitation bias over Bangladesh especially in
415 the southern and southeastern regions than in the Lowres and Highres simulations during JJAS
416 (Fig. 7 d, e, & f). The intensity of the precipitation bias is decreased in the Highres SST simulation
417 compared to the Highres coupled simulation over the southern and southeastern part of
418 Bangladesh. This suggests that the precipitation intensity bias is driven by the bias in the SST over
419 BOB.

420
421 Results show that the coupled model simulations (Lowres and Highres) have warmer SST over the
422 BOB compared to the observed SST (Fig. 8). This SST bias in the coupled CMCC CM2 runs
423 (Lowres and Highres) leads to a weaker land-sea thermal contrast that leads to a weaker LLJ (Fig.
424 8a, 8b). The bias in the 925 hPa circulation shows that wind anomalies are in the opposite direction
425 of the climatological summer monsoon LLJ circulation (Fig. 8a, 8b, 8d, & 8e). The prescribed SST
426 simulation (Highres SST) still shows a 925hPa wind bias. However, it overestimates the wind
427 speed compared to observations and contributes to the stronger moisture transport (Fig. 8c & 8f).
428 The moisture transport over Bangladesh is still underestimated in the Highres SST simulation.
429 Overall, seasonal mean precipitation is improved incrementally with a realistic representation of
430 the topography of the surrounding regions and climatological BOB SST variability.

431

432

433 **4. Discussion**

434

435 Bangladesh is in a unique geographical location in the tropical to the subtropical region that
436 receives most of its precipitation during the summer monsoon. Three regions of Bangladesh
437 receive maximum precipitations during the summer monsoon: northeastern (Sylhet division),
438 northwestern (northern Rangpur state near southern Himalaya), and southeastern (Chittagong
439 division) Bangladesh and surrounding regions. In this study, we have used three present-day
440 climate simulations of CMCC CM2 from CMIP6 experiments to understand the influence of local
441 topography and SST on summer monsoon precipitation over Bangladesh and its surrounding
442 regions. The Lowres coupled simulation uses a low atmospheric model resolution with a coarse
443 topography (1x1 degree). The Highres coupled simulation uses a relatively higher resolution
444 atmospheric model that uses a more realistic high-resolution topography (0.25x0.25 degree). The
445 Highres SST simulation uses the same atmospheric resolution as Highres simulation, except it has
446 a prescribed observed SST.

447
448 Precipitation maximum regions of Bangladesh are directly associated with the mountains of the
449 surrounding regions. The southern Himalayan Mountain range and Meghalaya Plateau block the
450 southwesterly wind that carries moisture and produces strong convergence that leads to
451 precipitation maxima. The band of the Arakan mountains acts as a local forcing to the precipitation
452 over the Myanmar region by blocking the low-level winds associated with the LLJ stream and
453 directly forcing local moisture convergence. However, the precipitation maxima over southeastern
454 Bangladesh (coastal region) are mostly due to inland moisture transports from BOB. Although
455 mountains play a crucial role in forcing the moisture to precipitate by convergence, the BOB plays
456 a significant role as a source of moisture for precipitation over Bangladesh. The moisture flux
457 divergence and 925hPa circulation revealed that the moisture content is carried from the northern
458 BOB by the LLJ circulation. During the summer monsoon, these winds are stronger due to a
459 monsoonal differential heating that creates a stronger land-sea thermal contrast and drives the
460 circulation with moisture content towards northern Bangladesh.

461
462 The CMCC CM2 model simulations show the influence of the topography and SST on summer
463 monsoon precipitation over Bangladesh. Compared to observations, the Lowres simulation shows
464 almost no peaks in the spatial distribution of precipitation over the northeastern part of Bangladesh
465 due to a lack of topographical features in the model. The Highres simulation has a better (higher

466 resolution) topography and simulates a better precipitation climatology than the Lowres. However,
467 the Highres coupled model simulation still shows significant precipitation bias over climatological
468 maximum precipitation regions of Bangladesh. The prescribed SST run (Highres SST) has
469 significantly less bias in the precipitation over Bangladesh compared to the coupled Lowres, and
470 Highres model runs. Interestingly, the pattern of the precipitation bias is very similar between the
471 Highres coupled, and the Highres prescribed SST run. The similarity in precipitation patterns
472 suggests that the pattern of precipitation bias is primarily due to local topography. In contrast, the
473 bias in magnitude is primarily due to the SST bias in the model.

474
475 The Highres and Highres SST model simulations still show significant precipitation bias compared
476 to observations. The maximum precipitation and moisture convergence region of northeastern
477 Bangladesh is especially shifted toward Indian states instead of Bangladesh, which creates a false
478 precipitation maximum. It suggests that the model still requires a more realistic high-resolution
479 topography to improve the simulation of precipitation climatology over Bangladesh, especially in
480 the northeastern region.

481
482 This study shows that the low-resolution model simulations can lead to a large monsoon
483 precipitation bias in regions like Bangladesh, where local topography plays a significant role. As
484 a result, a realistic SST simulation in the model alone is not enough to produce realistic monsoon
485 precipitation over Bangladesh and its surrounding regions. This suggests that a higher resolution
486 GCM with realistic topography can significantly improve the local climate prediction and climate
487 change projection.

488

489 **5. Conclusion**

490
491 We have analyzed CMCC-CM2 GCM simulations from CMIP6 experiments to understand the
492 importance of the local topography of surrounding mountains and SST in simulating summer
493 monsoon precipitation over Bangladesh and its surrounding regions. Our main results are
494 summarized as follows:

495

- 496 1. By analyzing observed data and CMCC-CM2 model simulations, our study shows that the
497 summer monsoon precipitation over Bangladesh is forced by the SST over BOB and
498 surrounding mountains near Bangladesh. The moisture content generated from the BOB
499 carried by the LLJ converges near local mountains to precipitate which creates three
500 distinct maximum precipitation regions over Bangladesh.
501
- 502 2. The climatological summer monsoon precipitation simulation of Bangladesh in a GCM is
503 sensitive to the choice of the horizontal resolution of the GCM simulation. Even with the
504 standard GCM model horizontal resolution (1x1 degree), the latest generation of climate
505 models fails to simulate. Overall, patterns and magnitudes of climatological precipitation
506 are improved in simulations with realistic local topography.
507
- 508 3. The BOB also plays a significant role as a source of moisture for precipitation over
509 Bangladesh. The prescribed SST run (Highres SST) has significantly less bias in the
510 precipitation over Bangladesh compared to the coupled Lowres and Highres model runs. It
511 implies that the SST in the BOB and tropical ocean system contributes to the summer
512 monsoon precipitation over Bangladesh.
513
514
- 515 4. Total area-averaged monthly mean precipitation, the peak of the seasonal cycle, onset,
516 cessation, and the length of the rainy seasons are improved in the Highres SST simulations
517 as compared to the Lowres, and Highres model simulations. This result suggests that the
518 SST of BOB drives the seasonal monsoon system over Bangladesh (Fig. 4).
519
- 520 5. Overall, our result suggests that the pattern of precipitation bias is primarily due to the local
521 topography. Whereas, the bias in the magnitude is primarily due to the SST bias in the
522 model.
523

524 The Highres SST simulations still produce a significant dry bias over Bangladesh even when
525 forced with the observed SST. This result shows that the CMCC CM2 model has less low-level
526 moisture content present over the BOB compared to observations during the summer monsoon.

527 Further investigation is needed to understand why the CMCC CM2 underestimates the summer
528 monsoon moisture content over the BOB.

529
530 In conclusion, the current study highlights the importance of higher spatial model resolution and
531 realistic representation of the BOB SST variability in climate models in reproducing the properties
532 of monsoon precipitation over Bangladesh and its surrounding regions.

533
534

535 **Acknowledgments**

536
537 We would like to thank Dr. Natalie J. Burls (George Mason University) for her initial contribution
538 to the idea of the manuscript.

539
540 **References**

- 541
542 Abdullah, A. Y. M., Bhuian, M. H., Kiselev, G., Dewan, A., Hasan, Q. K., & Rafiuddin, M.
543 (2020). Extreme temperature and rainfall events in Bangladesh: a comparison between
544 coastal and inland areas. *International Journal of Climatology*.
545 Acosta, R.P. and Huber, M., 2020. Competing topographic mechanisms for the summer Indo-
546 Asian monsoon. *Geophysical Research Letters*, 47(3), p.e2019GL085112.
547 Ahmed, M.K., Alam, M.S., Yousuf, A.H.M. and Islam, M.M., 2017. A long-term trend in
548 precipitation of different spatial regions of Bangladesh and its teleconnections with El
549 Niño/Southern Oscillation and Indian Ocean Dipole. *Theoretical and Applied Climatology*,
550 129(1), pp.473-486.
551 Ahmed, R. and Karmakar, S., 1993. Arrival and withdrawal dates of the summer monsoon in
552 Bangladesh. *International Journal of Climatology*, 13(7), pp.727-740.
553 Ahmed, T., Jin, H.G. and Baik, J.J., 2020. Spatiotemporal Variations of Precipitation in
554 Bangladesh Revealed by Nationwide Rain Gauge Data. *Asia-Pacific Journal of*
555 *Atmospheric Sciences*, 56(4), pp.593-602.
556 Alapaty, K., Raman, S., Mohanty, U.C. and Madala, R.V., 1995. Sensitivity of monsoon
557 circulations to changes in sea surface temperatures. *Atmospheric Environment*, 29(16),

- 558 pp.2139-2156.
- 559 Boos, W.R. and Kuang, Z., 2010. Dominant control of the South Asian monsoon by orographic
560 insulation versus plateau heating. *Nature*, 463(7278), pp.218-222.
- 561 Boos, W.R. and Hurley, J.V., 2013. Thermodynamic bias in the multimodel mean boreal summer
562 monsoon. *Journal of Climate*, 26(7), pp.2279-2287.
- 563 Breitenbach, S.F., Adkins, J.F., Meyer, H., Marwan, N., Kumar, K.K. and Haug, G.H., 2010.
564 Strong influence of water vapor source dynamics on stable isotopes in precipitation
565 observed in Southern Meghalaya, NE India. *Earth and Planetary Science Letters*, 292(1-2),
566 pp.212-220.
- 567 Chakraborty, A.N.R.S., Nanjundiah, R.S. and Srinivasan, J., 2006, September. Theoretical
568 aspects of the Onset of Indian summer monsoon from perturbed orography simulations in a
569 GCM. In *Annales Geophysicae* (Vol. 24, No. 8, pp. 2075-2089). Copernicus GmbH.
- 570 Chansaengkachang, K., Luadsong, A., & Ascharyaphohta, N. (2018). Vertically integrated
571 moisture flux convergence over Southeast Asia and its relation to rainfall over Thailand.
572 *Pertanika J Sci & Technol*, 26(1), 235-246.
- 573 Cherchi, A., Fogli, P.G., Lovato, T., Peano, D., Iovino, D., Gualdi, S., Masina, S., Scoccimarro,
574 E., Materia, S., Bellucci, A. and Navarra, A., 2019. Global mean climate and main patterns
575 of variability in the CMCC-CM2 coupled model. *Journal of Advances in Modeling Earth
576 Systems*, 11(1), pp.185-209.
- 577 Cherchi, A. and Navarra, A., 2007. Sensitivity of the Asian summer monsoon to the horizontal
578 resolution: differences between AMIP-type and coupled model experiments. *Climate
579 Dynamics*, 28(2-3), pp.273-290.
- 580 Cherchi, A., Kucharski, F. and Colleoni, F., 2018. Remote SST forcing on Indian summer
581 monsoon extreme years in AGCM experiments. *International Journal of Climatology*, 38,
582 pp.e160-e177.
- 583 Danielson, J.J. and Gesch, D.B., 2011. *Global multi-resolution terrain elevation data 2010
584 (GMTED2010)* (p. 26). US Department of the Interior, US Geological Survey.
- 585 Darand, M., & Pazhoh, F. (2019). Vertically integrated moisture flux convergence over Iran.
586 *Climate Dynamics*, 53(5), 3561-3582.
- 587 Eyring, V., S. Bony, GA Meehl, CA Senior, B. Stevens, RJ Stouffer, and KE Taylor, 2016.
588 Overview of the Coupled Model Intercomparison Project phase 6 (CMIP6) experimental

- 589 design and organization. *Geosci. Model Dev*, 9, pp.1937-1958.
- 590 Fasullo, J., & Webster, P. J. (2003). A hydrological definition of Indian monsoon onset and
591 withdrawal. *Journal of Climate*, 16(19), 3200-3211.
- 592 Feng, J., Li, J., Jin, F., Zhao, S. and Zhu, J., 2018. Relationship between the Hadley circulation
593 and different tropical meridional SST structures during boreal summer. *Journal of Climate*,
594 31(16), pp.6575-6590.
- 595 Feng, J. and Fu, C., 2006. Inter-comparison of 10-year precipitation simulated by several RCMs
596 for Asia. *Advances in atmospheric sciences*, 23(4), pp.531-542.
- 597 Funk, C., Verdin, A., Michaelsen, J., Peterson, P., Pedreros, D. and Husak, G., 2015. A global
598 satellite-assisted precipitation climatology. *Earth System Science Data*, 7(2), pp.275-287.
- 599 Gao, Y., Leung, L. R., Salathé Jr, E. P., Dominguez, F., Nijssen, B., & Lettenmaier, D. P. (2012).
600 Moisture flux convergence in regional and global climate models: Implications for droughts
601 in the southwestern United States under climate change. *Geophysical Research Letters*,
602 39(9).
- 603 George, G., Rao, D.N., Sabeerali, C.T., Srivastava, A. and Rao, S.A., 2016. Indian summer
604 monsoon prediction and simulation in CFSv2 coupled model. *Atmospheric Science Letters*,
605 17(1), pp.57-64.
- 606 Gill, A.E., 1980. Some simple solutions for heat-induced tropical circulation. *Quarterly Journal*
607 *of the Royal Meteorological Society*, 106(449), pp.447-462.
- 608 Goswami, B.B., Mukhopadhyay, P., Mahanta, R. and Goswami, B.N., 2010. Multiscale
609 interaction with topography and extreme rainfall events in the northeast Indian region.
610 *Journal of Geophysical Research: Atmospheres*, 115(D12).
- 611 Goswami, B.N., Rao, S.A., Sengupta, D. and Chakravorty, S., 2016. Monsoons to mixing in the
612 Bay of Bengal: Multiscale air-sea interactions and monsoon predictability. *Oceanography*,
613 29(2), pp.18-27.
- 614 Gu, H. and Wang, X., 2020. Performance of the RegCM4. 6 for High-Resolution Climate and
615 Extreme Simulations over Tibetan Plateau. *Atmosphere*, 11(10), p.1104.
- 616 Haarsma, R.J., Roberts, M.J., Vidale, P.L., Senior, C.A., Bellucci, A., Bao, Q., Chang, P., Corti,
617 S., Fučkar, N.S., Guemas, V. and Hardenberg, J.V., 2016. High resolution model
618 intercomparison project (HighResMIP v1. 0) for CMIP6. *Geoscientific Model Development*,
619 9(11), pp.4185-4208.

- 620 Hahn, D.G. and Manabe, S., 1975. The role of mountains in the south Asian monsoon
621 circulation. *Journal of Atmospheric Sciences*, 32(8), pp.1515-1541.
- 622 Hersbach, H., Bell, B., Berrisford, P., Hirahara, S., Horányi, A., Muñoz-Sabater, J., Nicolas, J.,
623 Peubey, C., Radu, R., Schepers, D. and Simmons, A., 2020. The ERA5 global reanalysis.
624 *Quarterly Journal of the Royal Meteorological Society*, 146(730), pp.1999-2049.
- 625 Kitoh, A., 2002. Effects of large-scale mountains on surface climate—A coupled ocean-
626 atmosphere general circulation model study. *Journal of the Meteorological Society of*
627 *Japan. Ser. II*, 80(5), pp.1165-1181.
- 628 Konduru, R.T. and Takahashi, H.G., 2020. Effects of Convection Representation and Model
629 Resolution on Diurnal Precipitation Cycle Over the Indian Monsoon Region: Toward a
630 Convection-Permitting Regional Climate Simulation. *Journal of Geophysical Research:*
631 *Atmospheres*, 125(16), p.e2019JD032150.
- 632 Kumar, K.N., Rajeevan, M., Pai, D.S., Srivastava, A.K. and Preethi, B., 2013. On the observed
633 variability of monsoon droughts over India. *Weather and Climate Extremes*, 1, pp.42-50.
- 634 Kripalani, R.H., Inamdar, S. and Sontakke, N.A., 1996. Rainfall variability over Bangladesh
635 and Nepal: Comparison and connections with features over India. *International Journal of*
636 *Climatology: A Journal of the Royal Meteorological Society*, 16(6), pp.689-703.
- 637 Lal, M., Meehl, G.A. and Arblaster, J.M., 2000. Simulation of Indian summer monsoon rainfall
638 and its intraseasonal variability in the NCAR climate system model. *Regional*
639 *Environmental Change*, 1(3-4), pp.163-179.
- 640 Legates, D.R., 2014. Climate models and their simulation of precipitation. *Energy &*
641 *environment*, 25(6-7), pp.1163-1175.
- 642 Lucas-Picher, P., Christensen, J.H., Saeed, F., Kumar, P., Asharaf, S., Ahrens, B., Wiltshire,
643 A.J., Jacob, D. and Hagemann, S., 2011. Can regional climate models represent the Indian
644 monsoon?. *Journal of Hydrometeorology*, 12(5), pp.849-868.
- 645 Medina, S., Houze Jr, R.A., Kumar, A. and Niyogi, D., 2010. Summer monsoon convection in
646 the Himalayan region: Terrain and land cover effects. *Quarterly Journal of the Royal*
647 *Meteorological Society: A journal of the atmospheric sciences, applied meteorology and*
648 *physical oceanography*, 136(648), pp.593-616.
- 649 Mishra, S.K., Sahany, S. and Salunke, P., 2017. Linkages between MJO and summer monsoon
650 rainfall over India and surrounding region. *Meteorology and Atmospheric Physics*, 129(3),

- 651 pp.283-296.
- 652 Montes, C., Acharya, N., Hassan, S.Q. and Krupnik, T.J., 2021. Intense precipitation events
653 during the monsoon season in Bangladesh as captured by satellite-based products. *Journal*
654 *of Hydrometeorology*, 22(6), pp.1405-1419.
- 655 Murata, F., Terao, T., Fujinami, H., Hayashi, T., Asada, H., Matsumoto, J. and Syiemlieh, H.J.,
656 2017. Dominant synoptic disturbance in the extreme rainfall at Cherrapunji, Northeast
657 India, based on 104 years of rainfall data (1902–2005). *Journal of Climate*, 30(20),
658 pp.8237-8251.
- 659 Nazrul Islam, M., Rafiuddin, M., Ahmed, A.U. and Kolli, R.K., 2008. Calibration of PRECIS in
660 employing future scenarios in Bangladesh. *International Journal of Climatology: A Journal*
661 *of the Royal Meteorological Society*, 28(5), pp.617-628.
- 662 Nowreen, S., Murshed, S.B., Islam, A.S., Bhaskaran, B. and Hasan, M.A., 2015. Changes of
663 rainfall extremes around the haor basin areas of Bangladesh using multi-member ensemble
664 RCM. *Theoretical and Applied Climatology*, 119(1), pp.363-377.
- 665 Ono, M. and Takahashi, H.G., 2016. Seasonal transition of precipitation characteristics
666 associated with land surface conditions in and around Bangladesh. *Journal of Geophysical*
667 *Research: Atmospheres*, 121(19), pp.11-190.
- 668 Oouchi, K., Noda, A.T., Satoh, M., Wang, B., Xie, S.P., Takahashi, H.G. and Yasunari, T., 2009.
669 Asian summer monsoon simulated by a global cloud-system-resolving model: Diurnal to
670 intra-seasonal variability. *Geophysical research letters*, 36(11).
- 671 Preethi, B., Kripalani, R.H. and Kumar, K.K., 2010. Indian summer monsoon rainfall variability
672 in global coupled ocean-atmospheric models. *Climate Dynamics*, 35(7), pp.1521-1539.
- 673 Privé, N.C. and Plumb, R.A., 2007. Monsoon dynamics with interactive forcing. Part I:
674 Axisymmetric studies. *Journal of the atmospheric sciences*, 64(5), pp.1417-1430.
- 675 Privé, N.C. and Plumb, R.A., 2007. Monsoon dynamics with interactive forcing. Part II: Impact
676 of eddies and asymmetric geometries. *Journal of the atmospheric sciences*, 64(5), pp.1431-
677 1442.
- 678 Prokop, P. and Walanus, A., 2015. Variation in the orographic extreme rain events over the
679 Meghalaya Hills in northeast India in the two halves of the twentieth century. *Theoretical*
680 *and Applied Climatology*, 121(1), pp.389-399.
- 681 Rafiuddin, M., Uyeda, H., & Islam, M. N. (2010). Characteristics of monsoon precipitation

- 682 systems in and around Bangladesh. *International Journal of Climatology: A Journal of the*
683 *Royal Meteorological Society*, 30(7), 1042-1055.
- 684 Rao, K.G. and Goswami, B.N., 1988. Interannual variations of sea surface temperature over the
685 Arabian Sea and the Indian monsoon: A new perspective. *Monthly Weather Review*, 116(3),
686 pp.558-568.
- 687 Ratna, S.B., Cherchi, A., Joseph, P.V., Behera, S.K., Abish, B. and Masina, S., 2016. Moisture
688 variability over the Indo-Pacific region and its influence on the Indian summer monsoon
689 rainfall. *Climate Dynamics*, 46(3-4), pp.949-965.
- 690 Rayner, N.A.A., Parker, D.E., Horton, E.B., Folland, C.K., Alexander, L.V., Rowell, D.P., Kent,
691 E.C. and Kaplan, A., 2003. Global analyses of sea surface temperature, sea ice, and night
692 marine air temperature since the late nineteenth century. *Journal of Geophysical Research:*
693 *Atmospheres*, 108(D14).
- 694 Rimi, R.H., Haustein, K., Barbour, E.J. and Allen, M.R., 2019. Risks of pre-monsoon extreme
695 rainfall events of Bangladesh: is anthropogenic climate change playing a role?. *Bull. Am.*
696 *Meteorol. Soc*, 100, pp.S61-S65.
- 697 Romatschke, U., Medina, S. and Houze, R.A., 2010. Regional, seasonal, and diurnal variations
698 of extreme convection in the South Asian region. *Journal of Climate*, 23(2), pp.419-439.
- 699 Roxy, M., 2014. Sensitivity of precipitation to sea surface temperature over the tropical summer
700 monsoon region—and its quantification. *Climate Dynamics*, 43(5-6), pp.1159-1169.
- 701 Salahuddin, A., Isaac, R.H., Curtis, S., and Matsumoto, J., 2006. Teleconnections between the
702 sea surface temperature in the Bay of Bengal and monsoon rainfall in Bangladesh. *Global*
703 *and Planetary Change*, 53(3), pp.188-197.
- 704 Seager, R., Ting, M., Held, I., Kushnir, Y., Lu, J., Vecchi, G., ... & Naik, N. (2007). Model
705 projections of an imminent transition to a more arid climate in southwestern North America.
706 *Science*, 316(5828), 1181-1184.
- 707 Shukla, J., 1981. Dynamical predictability of monthly means. *Journal of Atmospheric Sciences*,
708 38(12), pp.2547-2572.
- 709 Singh, B., Cash, B. and Kinter III, J.L., 2019. Indian summer monsoon variability forecasts in
710 the North American multimodel ensemble. *Climate Dynamics*, 53(12), pp.7321-7334.
- 711 Sugimoto, S. and Takahashi, H.G., 2017. Seasonal differences in precipitation sensitivity to soil
712 moisture in Bangladesh and surrounding regions. *Journal of Climate*, 30(3), pp.921-938.

- 713 Syed, F.S., Iqbal, W., Syed, A.A.B. and Rasul, G., 2014. Uncertainties in the regional climate
714 models simulations of South-Asian summer monsoon and climate change. *Climate*
715 *Dynamics*, 42(7-8), pp.2079-2097.
- 716 Ullah, K., & Gao, S. (2012). Moisture transport over the Arabian Sea associated with summer
717 rainfall over Pakistan in 1994 and 2002. *Advances in Atmospheric Sciences*, 29(3), 501-
718 508.
- 719 Wahiduzzaman, M. and Luo, J.J., 2021. A statistical analysis on the contribution of El Niño–
720 Southern Oscillation to the rainfall and temperature over Bangladesh. *Meteorology and*
721 *Atmospheric Physics*, 133(1), pp.55-68.
- 722 Xie, S. P., Xu, H., Saji, N. H., Wang, Y., & Liu, W. T. (2006). Role of narrow mountains in
723 large-scale organization of Asian monsoon convection. *Journal of climate*, 19(14), 3420-
724 3429.
- 725 Yang, Y., Zhao, T., Ni, G. and Sun, T., 2017. Atmospheric rivers over the Bay of Bengal lead to
726 northern Indian extreme rainfall. *International Journal of Climatology*, 38(2), pp.1010-
727 1021.
- 728 Yanai, M. and Li, C., 1994. Mechanism of heating and the boundary layer over the Tibetan
729 Plateau. *Monthly Weather Review*, 122(2), pp.305-323.

Figures:

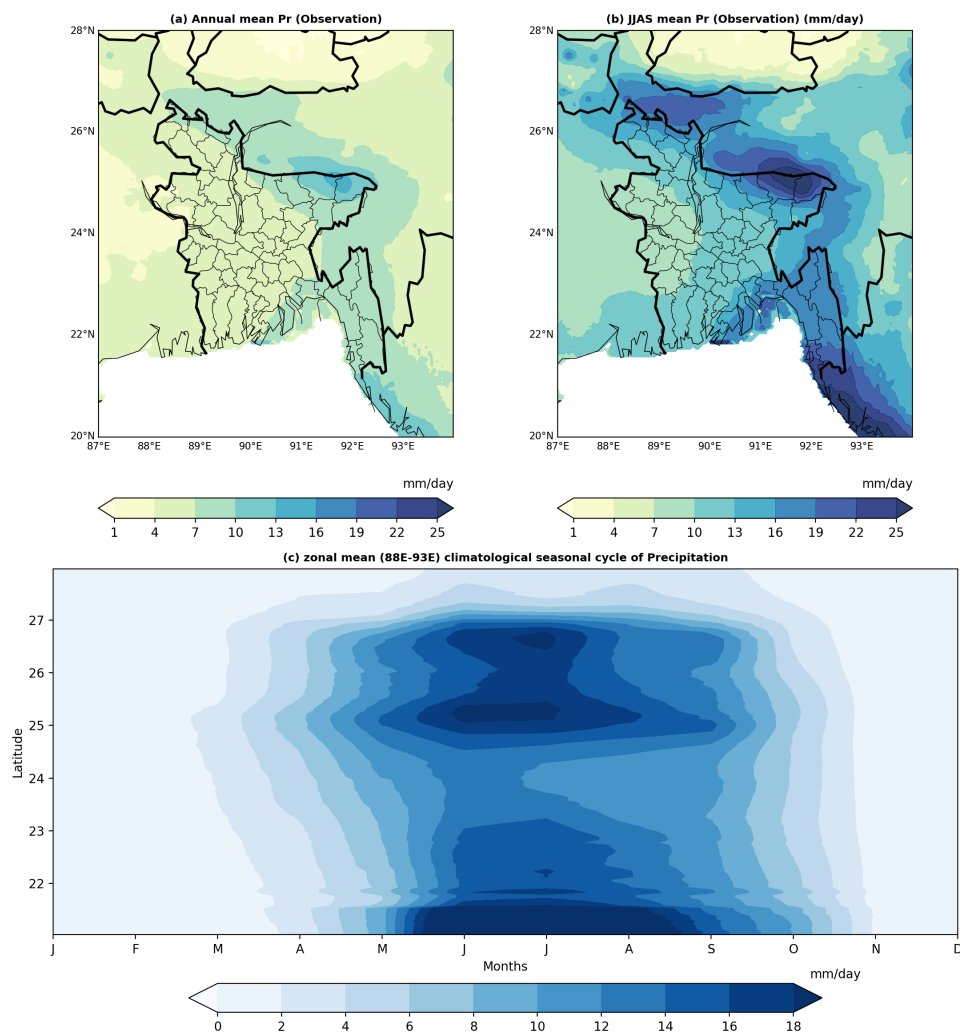


Fig. 1 Precipitation climatology (years 1981-2014) of (a) Annual mean, (b) JJAS mean, and (c) zonal mean (average over 88E-93E) seasonal cycle of Chirps v2 observed data as a function of latitude (units: mm/day).

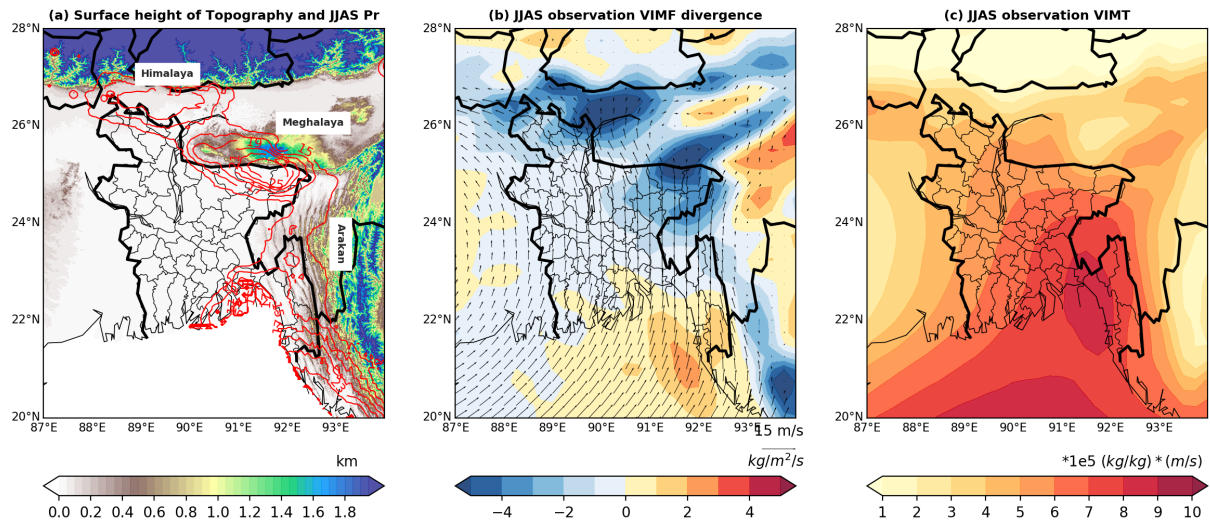


Fig. 2 (a) Height of topography of Bangladesh and its surrounding regions (units: km), and the JJAS observed precipitation is contoured as red lines in mm/day. (b) JJAS mean ERA-5 vertically integrated moisture flux (VIMF) divergence (1000-700 hPa) (units: $\text{kg/m}^2/\text{s}$) is shown in shaded color, and 850hPa wind circulation is shown as a vector (units: m/s) (years mean 1981-2014). VIMF positive values show divergence, and negative values show the convergence of vertically integrated winds. (c) JJAS mean ERA-5 vertically integrated moisture transport (VIMT) (1000-700 hPa) (units: $10^5 \cdot \text{kg/kg} \cdot \text{m/s}$)

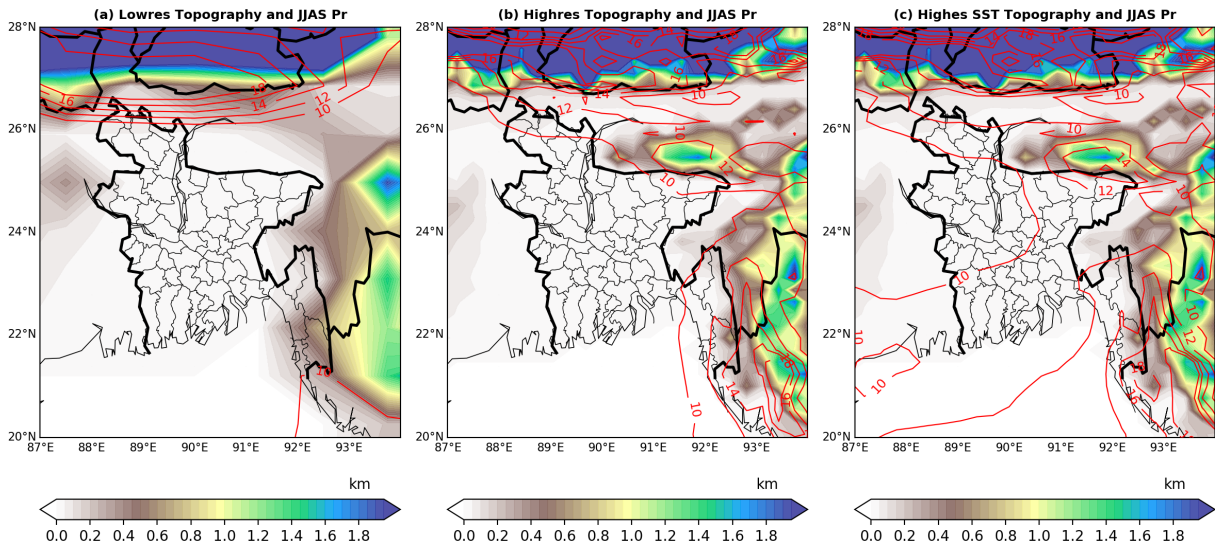


Fig. 3 Model topography in shaded color and 34 years (1981-2014) JJAS mean precipitation contoured in red-colored for (a) Lowres, (b) Highres, and (c) Highres SST (units: mm/day). The topography map shows no existence of the Meghalaya Plateau on the CMCC CM2 Lowres simulation.

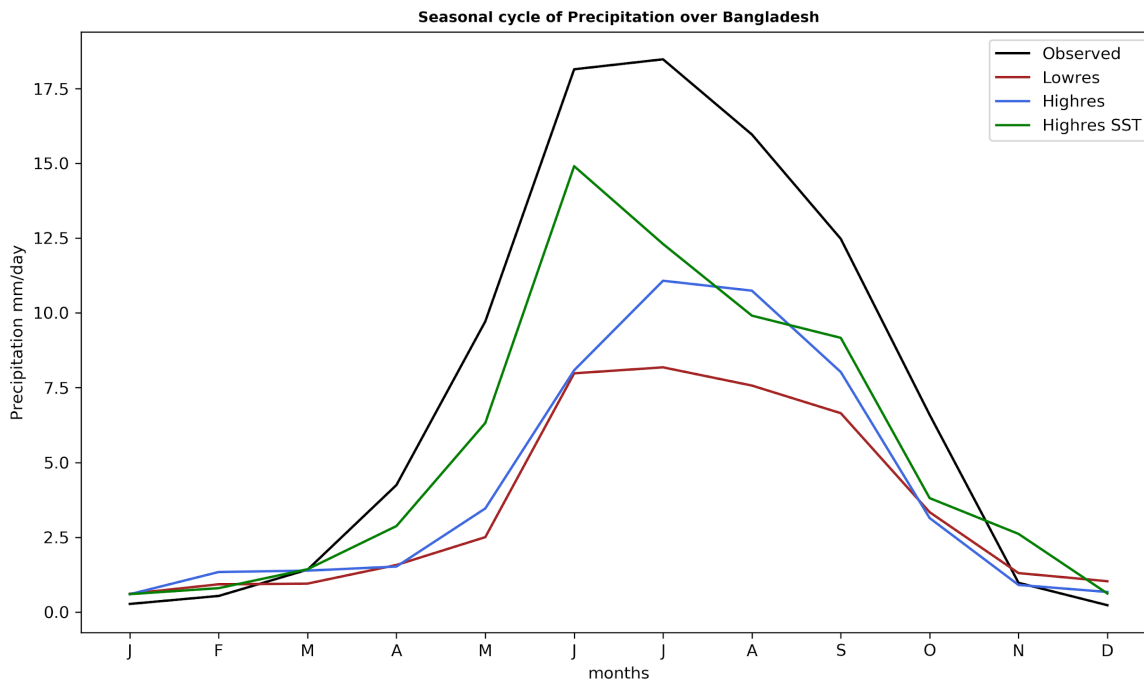


Fig. 4 Climatological (mean over 1979-2014) monthly seasonal cycle of precipitation over Bangladesh is shown for observation (black colored), CMCC CM2 Lowres (brown colored), CMCC CM2 Highres (blue colored), and CMCC CM2 Highres SST (green colored) (units: mm/day).

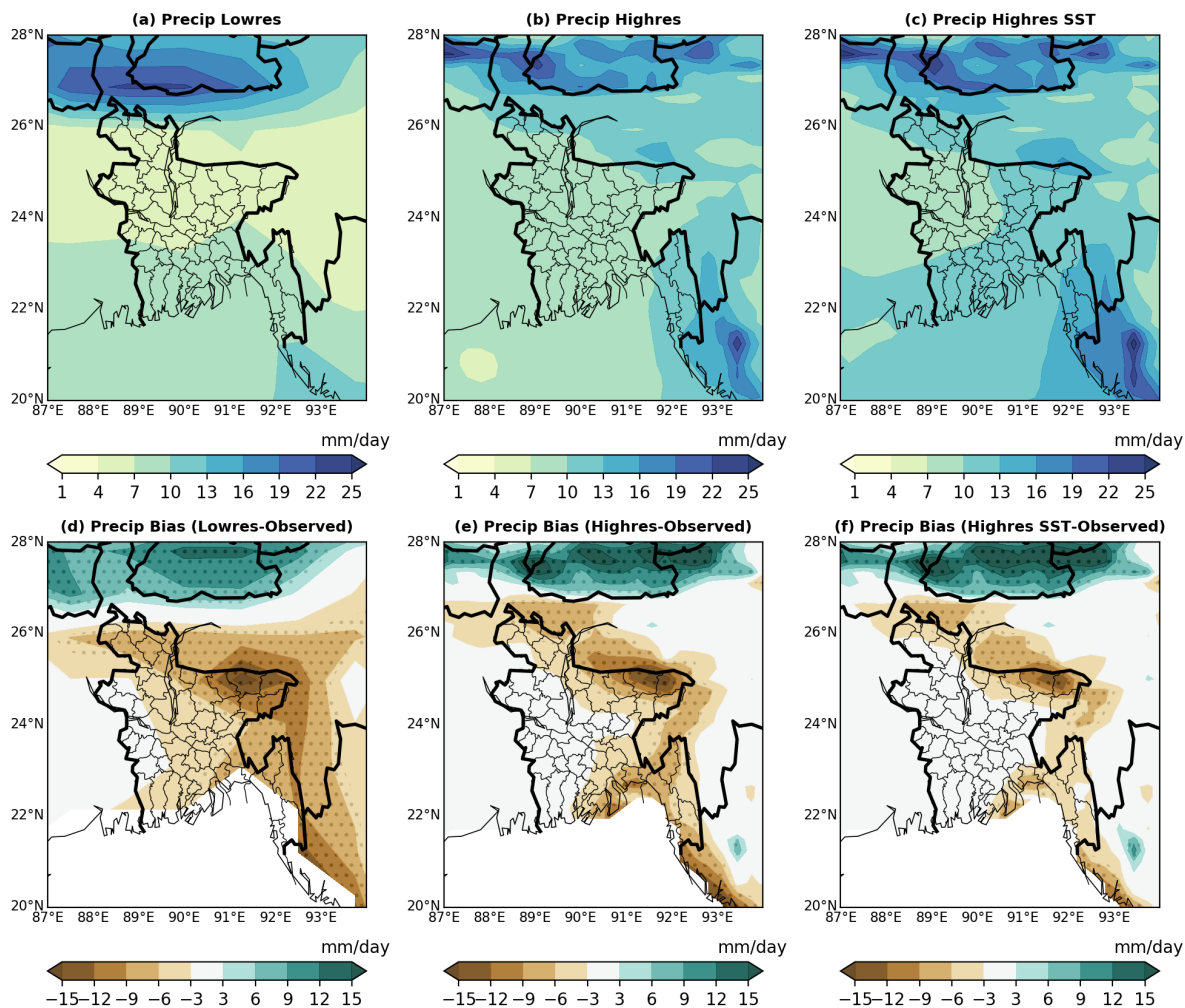


Fig. 5 JJAS mean precipitation climatology of CMCC CM2 for (a) Lowres, (b) Highres, and (c) Highres SST (units: mm/day). The precipitation bias in the CMCC CM2 simulations is shown for (d) Lowres - Observed, (e) Highres - Observed, and (f) Highres SST - Observed. Units are in mm/day. Precipitation bias plots are stippled at a 95% significance level calculated using a 2-sided student t-test for the difference of means.

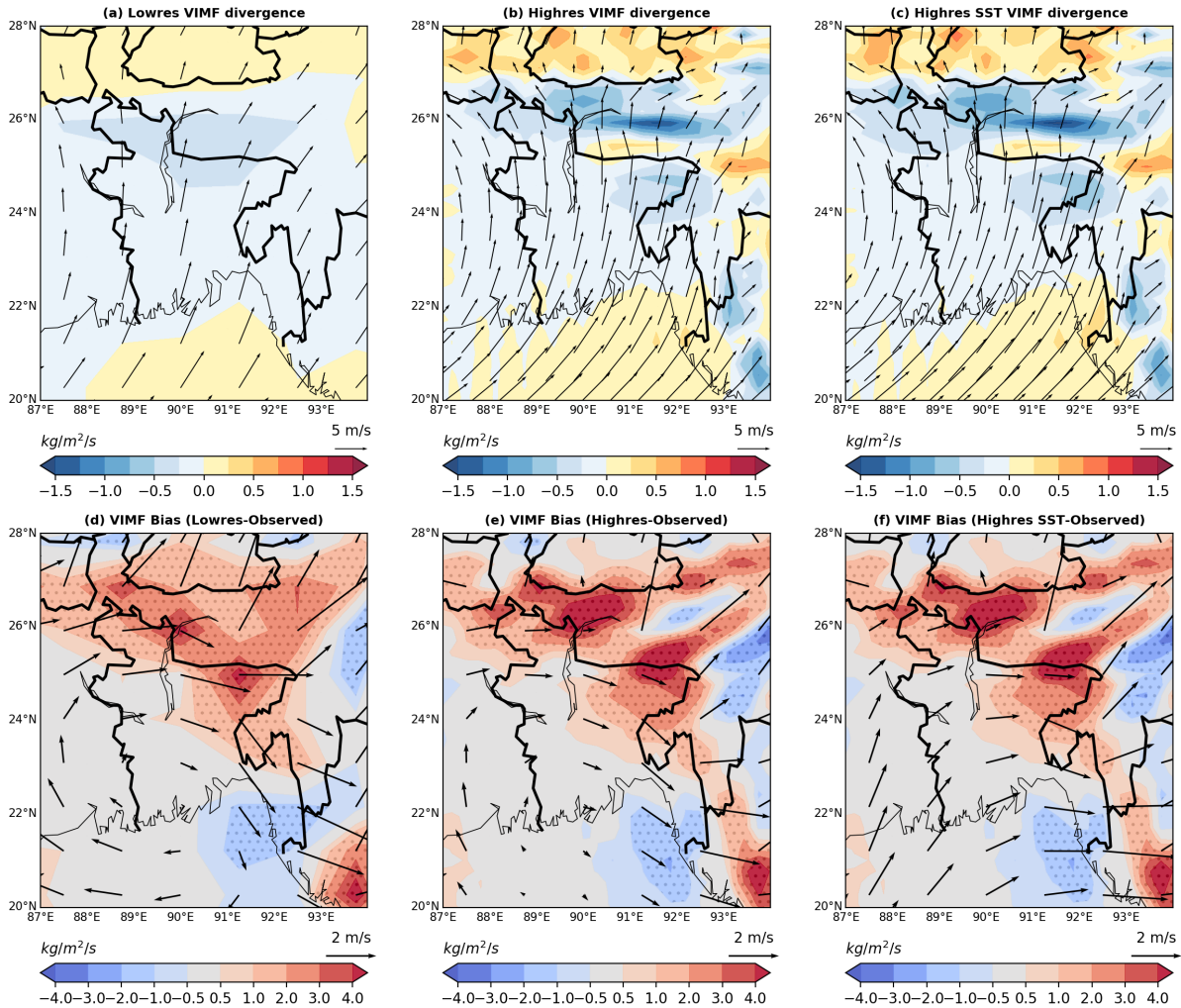


Fig. 6 JJAS mean climatological mean (1981-2014) vertically integrated moisture flux convergence (VIMF) (1000-700hPa) (units: $\text{kg/m}^2/\text{s}$) shown as shaded color and 925hPa wind circulation (units: m/s) shown as vector for CMCC CM2 (a) Lowres, (b) Highres, and (c) Highres SST. The VIMF bias (as shaded color) (units: $\text{kg/m}^2/\text{s}$) and 925hPa wind bias (units: m/s) (as vector) in the model simulation compared to observation is shown for (d) Lowres - Observation, (e) Highres - Observation, and (f) Highres SST - Observation. VIMF bias differences are stippled at a 95% significance level calculated using a 2-sided student t-test for the difference of means.

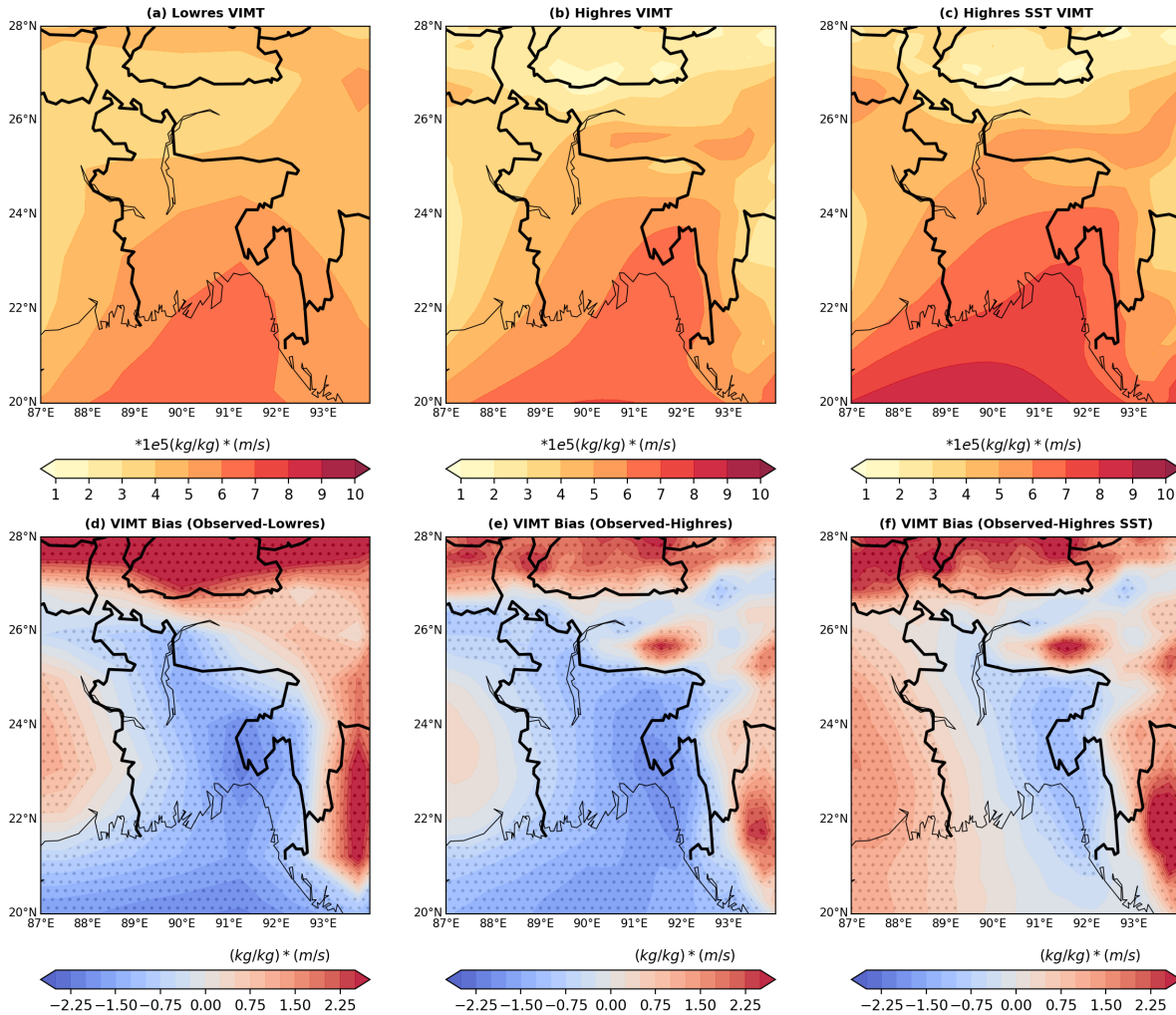


Fig. 7 JJAS means climatological vertically integrated moisture transport (VIMT) is shown for (a) Lowres, (b) Highres, and (c) Highres SST (units: 10^5 kg/kg * m/s). The VIMT bias (units: kg/kg * m/s) in the model simulation compared to observation is shown for (d) Lowres - Observation, (e) Highres - Observation, and (f) Highres SST - Observation. VIMT bias differences are stippled at a 95% significance level calculated using a 2-sided student t-test for the difference of means.

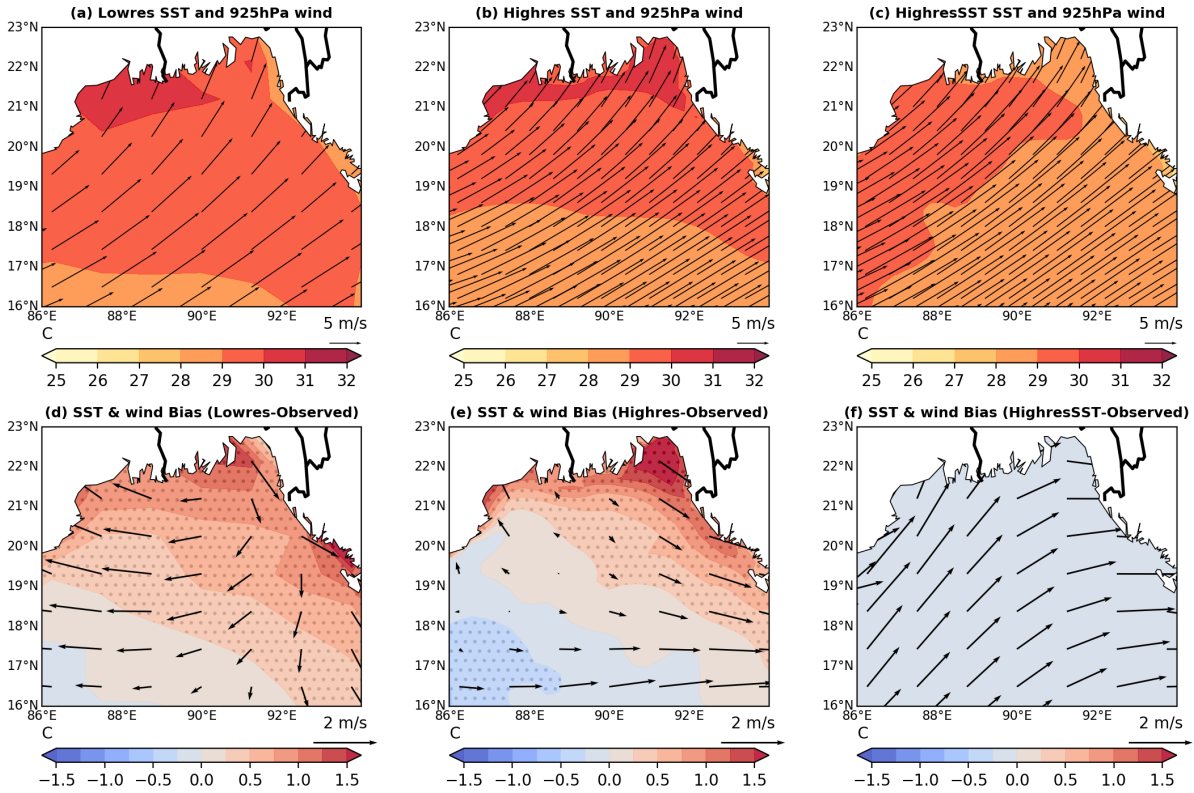


Fig. 8 JJAS climatological mean (1981-2014) SST for CMCC CM2 (a) Lowres, (b) Highres, and (c) Highres SST. The SST bias (units: C) and 925hPa wind bias (units: m/s) (as vector) in the model simulation compared to observation is shown for (d) Lowres - Observation, (e) Highres - Observation, and (f) Highres SST - Observation. SST bias differences are stippled at a 95% significance level calculated using a 2-sided student t-test for the difference of means.